ACS APPLIED MATERIALS & INTERFACES

RESEARCH ARTICLE

www.acsami.org

Wettability Control of ZnO Nanoparticles for Universal Applications

Mikyung Lee, Geunjae Kwak, and Kijung Yong*

Surface Chemistry Laboratory of Electronic Materials (SCHEMA), Department of Chemical Engineering, POSTECH, Pohang 790-784, Korea

Supporting Information

ABSTRACT: Herein, a facile approach for the fabrication of a superhydrophobic nanocoating through a simple spin-coating and chemical modification is demonstrated. The resulting coated surface displayed a static water contact angle of 158° and contact angle hysteresis of 1°, showing excellent superhydrophobicity. The surface wettability could be modulated by the number of ZnO nanoparticle coating cycles, which in turn affected surface roughness. Because of its surface-independent characteristics, this method could be applicable to a wide range of substrates including metals, semiconductors, papers, cotton fabrics, and even flexible polymer substrates. This superhydrophobic surface showed high stability in thermal and dynamic conditions, which are essential elements for practical applications. Furthermore, the reversible switching of wetting behaviors from the superhydrophilic state to the superhydrophobic state was demonstrated using repeated chemical modification/heat treatment cycles of the coating films.

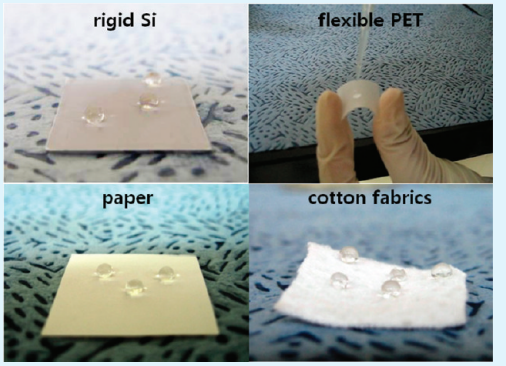

KEYWORDS: superhydrophobic, surface modification, flexible substrate, wettability control, thermal stability, impact dynamics

INTRODUCTION

Surface-wetting behaviors have recently attracted significant attention due to their potential application in a variety of areas.[1−5] Surface wettability is governed by surface roughness and chemical composition; increasing surface roughness and lowering surface energy can remarkably enhance surface water repellency. In superhydrophobic conditions, a water droplet sits unstably on top of the superhydrophobic surface, forming a spherical shape with a contact angle greater than 150° and rolls away quickly when subjected to gentle vibration. This phenomenon is easily exemplified by the lotus leaf, thus called the "lotus effect".[6] Inspired by natural superhydrophobicity, artificial superhydrophobic surfaces have been obtained by building a rough topography and modifying the surface by chemical coating with low surface-energy molecules.

In the past few decades, many attempts to fabricate superhydrophobic surfaces have been inspired by mimicking nature. Various one-dimensional nanomaterials with inherent shapes resembling the papillae of the lotus leaf have been used to construct superhydrophobic surfaces, including ZnO,[7−10] TiO_2,[11−13] WO_x,[14,15] SiC nanowires,[16,17] and carbon nanotubes.[18−20] In general, these 1-D nanomaterials are grown directly on the substrates to ensure vertical alignments, demonstrating they are strongly influenced by the substrate materials. Moreover, in many cases, the preparation process involves strict growth conditions such as a high temperature, harsh chemical treatments, and complex processing techniques.

One of the smart approaches to overcome these restrictions imposed on the substrate is coating the substrate surface with functionalized nanoparticles. Recently, fabrication of superhydrophobic surfaces covered with nanoparticles has been developed, using a variety of substrates, including glass and cotton fabric. Generally, the nanoparticle materials applied are limited to SiO_2[21−25] and few studies have been demonstrated for other nanoparticle materials for this use. Moreover the nanoparticle coating methods necessitate a repetitive layer-by-layer process and require tedious template removal steps via chemical etching or calcinations. Recently Severtson et al.[26] reported the fabrication of a superhydrophobic surface by using a $ZnO_{coating}$/$PDMS_{substrate}$ composite film, which showed superoleophilicity with recovery of superhydrophobicity after oil fouling. However, these properties originate from the material properties of the substrate (PDMS) itself, demonstrating its restriction in selection of the substrate materials again.

We report, herein, a facile method for fabricating superhydrophobic surfaces, applicable for a wide range of substrates, by spin-coating of ZnO nanoparticles (NPs) onto a surface with chemical modifications. The surface wettability could be controlled by the number of ZnO NP coating cycles, in turn affecting the surface roughness. Because the deposition of ZnO NPs is surface-independent, this method could be generally applicable to various substrates, including metals, semiconductors, paper, cotton fabric, and even flexible substrates. Moreover, this coating layer demonstrated good thermal stability over 200 °C,

Received: April 15, 2011
Accepted: August 5, 2011
Published: August 05, 2011

dx.doi.org/10.1021/am2004762 | ACS Appl. Mater. Interfaces 2011, 3, 3350–3356

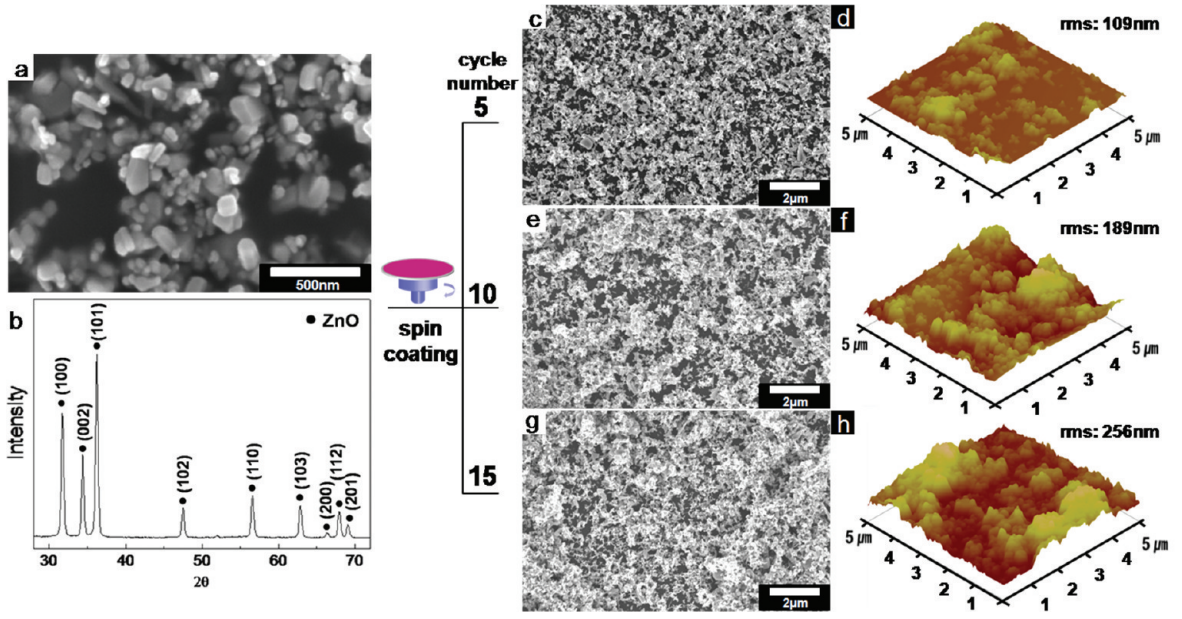

Figure 1. (a) SEM image and (b) XRD spectrum of ZnO nanoparticles used for spin-coating. (c, e, g) Magnified SEM images of coating films as prepared by deposition of 5, 10, and 15 cycles, respectively. (d, f, h) AFM images corresponding to samples e, d, and g, respectively.

suggesting its potential for industrial applications. The extreme wetting transition between the superhydrophobic and superhydrophilic states was completely switchable upon coating with or removal of the hydrophobic molecules at elevated temperatures. Additionally, we demonstrated the impact dynamics of a water droplet to characterize how the surface energy influences the drop impact transitions.

EXPERIMENTAL SECTION

Materials. Zinc oxide (ZnO) NPs and stearic acid ($CH_3(CH_2)_{16}$-COOH) were purchased from Aldrich and used without additional purification. Absolute ethanol was obtained from Fisher and used as received. Silicon and polyethylene terephthalate (PET) substrates were supplied from Shinetsu and Aldrich, respectively. Paper and cotton fabrics were purchased from a general store.

Preparation of Superhydrophobic ZnO Surface. ZnO NPs (0.07 g) dissolved in 50 mL of absolute ethanol were vigorously stirred at room temperature for 24 h. The colloidal suspension was continuously stirred prior to its use to prevent agglomeration of the particles. The solution was spin-coated onto the silicon substrate surface at 500 rpm for 10 s and dried on a hot plate for 1 min. This process was repeated 15 times. After deposition, the previously prepared substrate was immersed into a 5 mmol solution of stearic acid dissolved in ethanol for 15 min. After dip-coating of stearic acid, the samples were gently blown dry with N_2.

The adhesion was enhanced through repetitive drying processes between spin coatings. Without drying processes, the particles on the surface cannot withstand the surface modification; upon dipping the ZnO NP films into the solution of stearic acid there are loss of the ZnO NPs as a consequence of dissolving into the solution. With drying processes, however, the ZnO NPs can bear the surface modification and maintain their superhydrophobicity even after exposure to ambient air for several months.

Characterization. The chemical composition of the samples was analyzed using X-ray photoelectron spectra (XPS) using monochromatic Mg Kα radiation as the X-ray source. The surface morphology of coated samples was characterized by both field-emission scanning electron microscopy (FE-SEM) and scanning probe microscopy (SPM). FE-SEM images were obtained on a XL30S FEG (Philips, The Netherlands) at an accelerating voltage of 5 kV. Scanning prove microscopy (SPM) images were taken on a PUCO Station STD (GmbH, Germany). The room-temperature photoluminescence (PL) spectra were recorded using a FP-6500 fluorescence spectrophotometer (JASCO, U.K.). Fourier transform infrared (FTIR) spectroscopy was performed with a Nicolet6700 FTIR spectrometer (Thermo Scientific). The surface-wetting properties were evaluated using a SEO300A contact angle system (SEO, South Korea). The water contact angle of the surface was measured by the sessile drop method at several different positions on each sample using 7 μL droplets of deionized water; the mean values are reported in this paper. The advancing and receding contact angles were measured during the growth and shrinkage of a droplet, respectively. The dynamic impact behaviors of droplets were recorded using a high-speed camera (Photron) at 2 000 frames per second.

RESULTS AND DISCUSSION

In the current work, we applied the spin-coating of ZnO NPs as the main deposition method to fabricate superhydrophobic surfaces. Surface wettability could be controlled by varying the number of spin-coating cycles of the ZnO/ethanol colloidal suspension. Figure 1a shows an FE-SEM image of ZnO NPs used for coating. As-prepared ZnO NPs ranged in size from below 10 nm to several hundreds of nanometers. The large distribution of particle sizes produces a rough coated substrate surface, thus affecting its superhydrophobicity. XRD analysis, shown in Figure 1b, revealed that all diffraction peaks could be assigned to ZnO and monophasic zincite with a hexagonal structure was produced as a product. (JCPDS card: 36-1451).

After spin-coating ZnO NPs on the silicon substrate, the morphological changes were observed by FE-SEM depending on the number of coating cycles (Figure 1). The surface morphologies resulting from 5, 10, and 15 coating cycles are shown in Figure 1c,e,g, with corresponding AFM images in Figure 1d,f,h, respectively. As seen in these figures, the uniformity and the areal number density of ZnO NPs increased upon increasing the

number of deposition cycles. SEM and AFM images clearly showed that sparsely formed ZnO NP islands at the initial stages of low deposition cycles coalesce together to form bigger islands with a higher roughness upon increasing the number of coating cycles. This trend increased the surface roughness (rms) of a coated surface for 15 and less coating cycles. On the contrary, surfaces exposed to over 20 coating cycles exhibited a decrease in surface roughness due to the filling of the deep valleys produced by the ZnO NPs.

Surface wettability was tested on as-prepared ZnO NP coated surfaces. Irrespective of the number of coating cycles, all surfaces showed superhydrophilic properties with a water contact angle (CA) below 5°. Because the ZnO surface is terminated with hydroxyl groups at the current deposition conditions, resulting in a hydrophilic surface.[27] However, after chemical modification of the ZnO surface with a self-assembled monolayer (SAM) coating of stearic acid, the surface wettability drastically changed into a superhydrophobic state.

The surface wettability was evaluated by measuring the water contact angle and contact angle hysteresis, a difference between advancing and receding contact angle. Figure 2a shows a comparison of the water contact angles of the chemically modified ZnO NP surfaces as a function of deposition cycles, 5, 10, 15, and 20 cycles. The water contact angle increased steadily upon increasing the number of deposition cycles up to 15 cycles (158°) but it decreased slightly after 20 coating cycles (151°). These trends agree well with the tendency of its rms values. Similarly, the roughness increased monotonically up to 15 coating cycles and then fell after 20 coating cycles. These results confirmed that the surface wettability is closely related to the surface roughness.

The contact angle hysteresis is also related to the surface roughness and adhesion to the surface. The advancing contact angle and contact angle hysteresis as a function of 5, 10, 15, and 20 deposition cycles are shown in Figure 2b. The magnitude of contact angle hysteresis decreased drastically with increasing the number of ZnO NP deposition cycles. For ZnO films exposed to less than five coating cycles, the water droplet strongly stuck to the surface and did not fall even when the substrate was turned upside down. The water droplet was expected to easily penetrate into the free space between the valleys and pinned on the substrate with high water adhesion (Figure 2c, left). The Wenzel wetting state[28] can be expressed as

$$\cos\theta^* = r\cos\theta \quad (1)$$

Here, θ^* and θ are the water contact angles for textured and flat surfaces, respectively, and r is surface roughness ($r \geq 1$). From the Wenzel wetting state, as the surface roughness increased, the solid−liquid contact area increased, leading to a large contact angle hysteresis. For ZnO films with more than 10 coating cycles, however, the contact angle hysteresis was almost 0°, showing superhydrophobicity. The water droplet rolled off rapidly when the surface was slightly tilted, consistent with the Cassie and Baxter superhydrophobic behavior (Figure 2c, right). According to the Cassie and Baxter model,[29] the water contact angle on the nanostructured surface is greatly influenced by the surface fraction of solid (f_1) versus air pockets (f_2), in which the sum of these two parameters is 1 (i.e., $f_1 + f_2 = 1$):

$$\cos\theta^* = f_1\cos\theta - f_2 \quad (2)$$

In this Cassie and Baxter wetting state, the large volume of air trapped between the valleys prevents the water droplet from penetrating into the free space and the water droplet is suspended above the substrate unstably. Equation 2 reveals that as the volume of air trapped between valleys increases (decreasing f_1), the surface shows more hydrophobicity (increasing θ^*). Stearic acid modification of the ZnO film with sufficient roughness to produce superhydrophobicity showed a reduced surface energy, yielded a low solid surface fraction (f_1) and a high air-surface fraction (f_2), resulting in a large water contact angle. According to eq 2, the values of f_1 were calculated to be 0.466, 0.126, and 0.386 for 10, 15, and 20 coating cycles, respectively, which is the reverse trend displayed by the water contact angles. This result indicates that the fraction of air pockets plays a primary role in superhydrophobic behavior.

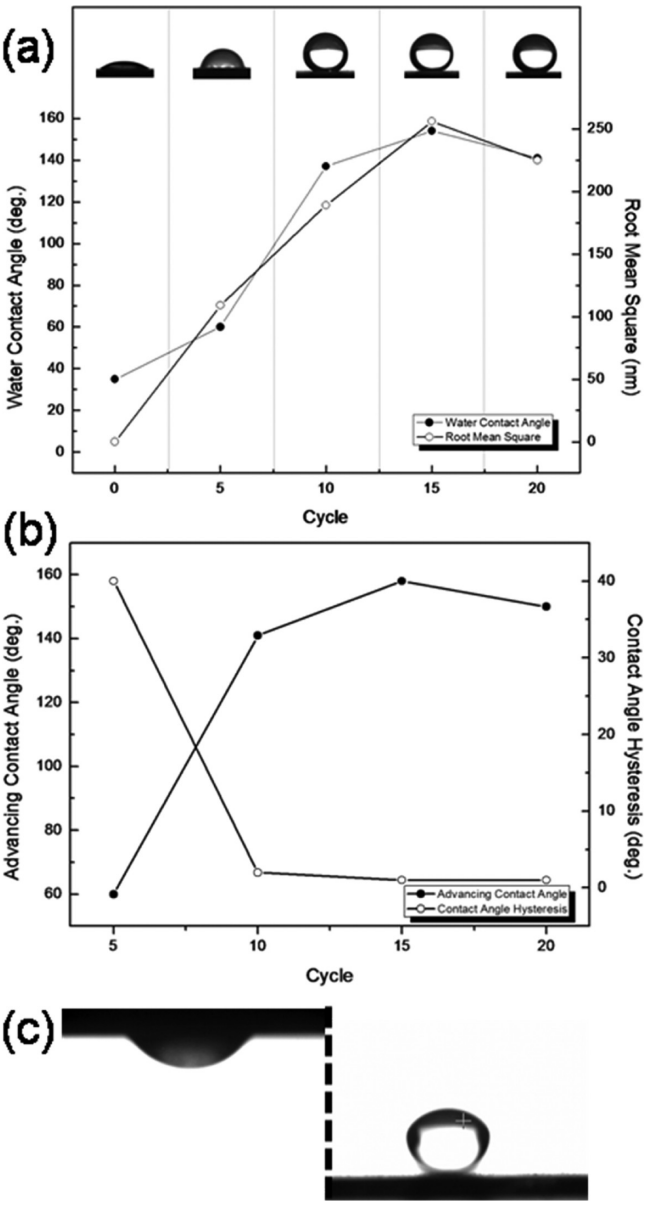

Figure 2. (a) Variations in the water contact angles of the ZnO nanoparticle-coated surfaces treated with stearic acids as a function of 0, 5, 10, 15, and 20 deposition cycles, (b) advancing contact angles and contact angle hysteresis as a function of 5, 10, 15, and 20 deposition cycles, (c) images of the static water contact angle (left) and sliding angle (right) of ZnO coatings prepared by 5 and 10 deposition cycles, respectively.

To test the effects of carbon chain length of fatty acids, as-prepared ZnO NP films were treated with different kinds of fatty acids, such as hexanoic acid (C = 6), dodecanoic acid (C = 12), and stearic acid (C = 18). The water contact angle of fatty acid modified ZnO NP films increased monotonically with increasing the carbon number of fatty acids as shown in Figure 3.

This simple coating method using ZnO NPs is easily extendable to various substrate materials without limitation. Figure 4 shows photographs of water droplets on various substrates: rigid Si, flexible PET, paper, and cotton fabrics. Regardless of the substrate materials, the use of our simple ZnO NP deposition with the chemical modification method results in a stable superhydrophobic state of surfaces with high water contact angles.

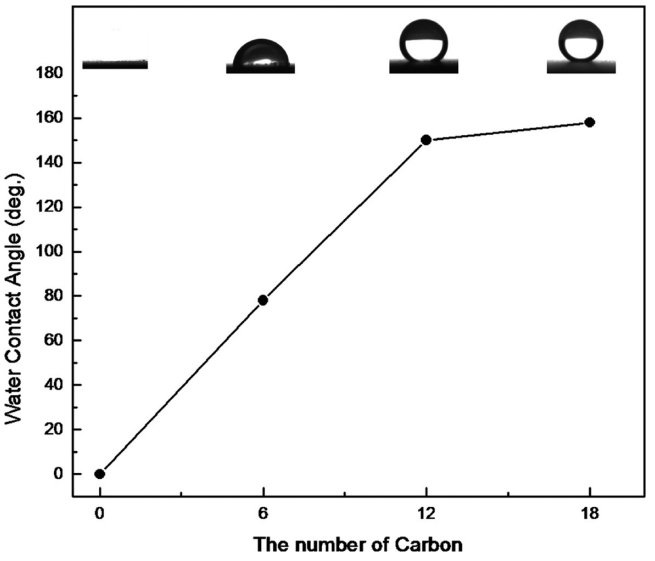

Figure 3. Water contact angle of fatty acid modified ZnO NP films as a function of the carbon number of fatty acids. ZnO NP films were prepared by 15 cycles of spin coating deposition.

To obtain a superhydrophobic surface, both the microstructure of the ZnO NPs and stearic acid adsorption layers are required. The adsorption of stearic acid on the surface without ZnO NPs does not produce the superhydrophobicity (Supporting Information, Table S1).

Because our fabrication method of superhydrophobicity uses the chemisorption of stearic acid SAMs, the thermal stability of the superhydrophobicity is strongly dependent on the chemical stability of the stearic acid upon heat treatment. To test the thermal stability of the superhydrophobic surfaces, chemically modified ZnO NPs films were air-annealed for 30 min at various temperature conditions (Figure 5a). The superhydrophobicity was stably maintained up to 240 °C, but a drastic transition from the superhydrophobic to superhydrophilic state was observed in the case of annealing temperature going over 240 °C. When the sample was annealed for 30 min at 300 °C, the water contact angle decreased to almost 0°, as observed in as-prepared ZnO NPs film. This sharp conversion into a hydrophilic state is hypothesized to be due to the thermal decomposition of stearic acid molecules in this temperature range. The thermal decomposition of stearic acid was confirmed by XPS (Figure 5b) and Fourier transform-infrared (FT-IR) analysis (Figure 5c). XPS spectra of superhydrophobic surfaces measured after heat treatment at various annealing temperatures showed that C 1s peak intensity of stearic acid was maintained up to 200 °C but rapidly decreased upon annealing at 300 °C. These results indicate that carbon chains of stearic acid thermally decomposed in this temperature range, which exposed the ZnO NPs to the exterior surface. FT-IR spectra of stearic acid-modified ZnO NPs film confirmed these XPS analysis results. The peak at wavenumber 2954 cm^{-1} was ascribed to the asymmetric C−H stretching mode of the $-CH_3$ group, and the two peaks at 2923 and 2850 were attributed to the asymmetric and symmetric C−H stretching modes of $-CH_2$ groups of stearic acid, respectively. A drastic decrease in intensity of the three peaks was observed resulting from thermal decomposition of stearic acid molecules. The effects of thermal annealing on the crystalline defects of ZnO NPs were also studied using photoluminescence, and

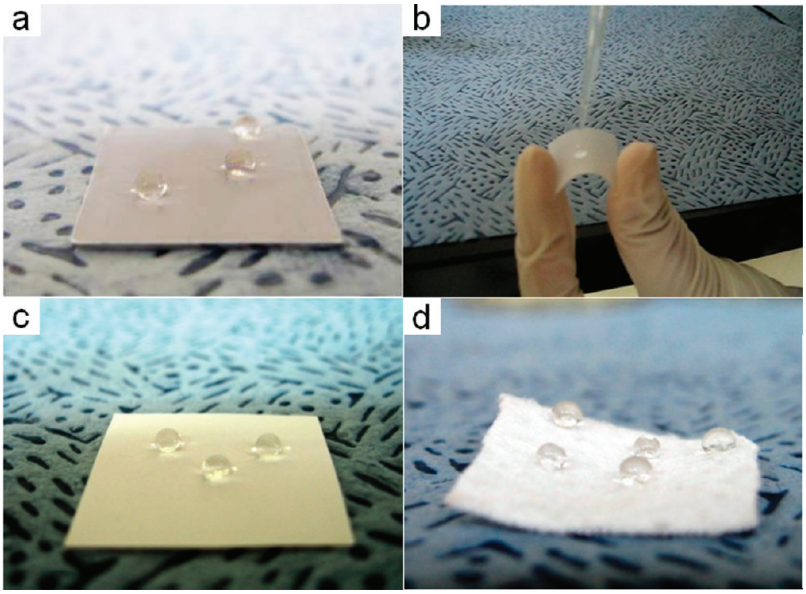

Figure 4. Photographs of various surfaces demonstrating superhydrophobicity: (a) Si substrate, (b) PET film, (c) paper, and (d) cotton fabrics.

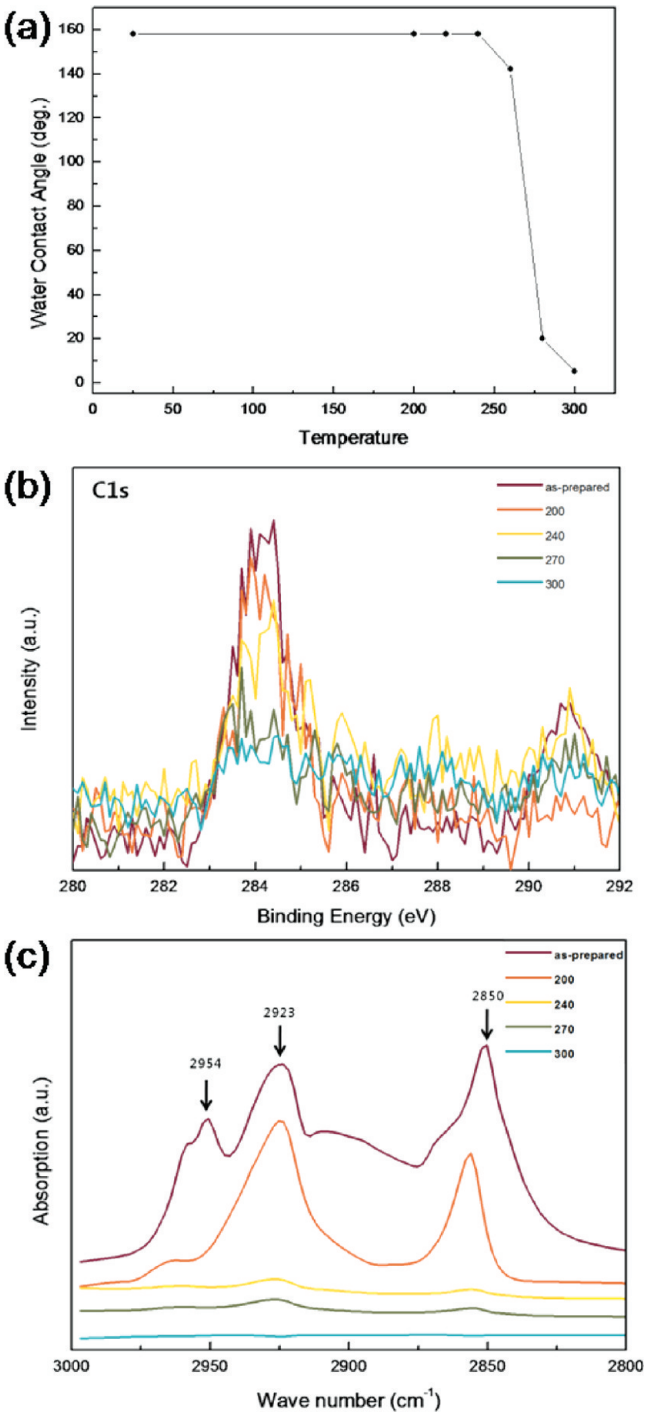

Figure 5. (a) Temperature dependence of water contact angle on stearic acid-treated ZnO NPs films, (b) XPS spectra of C 1s, and (c) FT-IR spectra showing $-CH_n$ peaks of stearic acid-modified ZnO NPs film at various annealing temperatures in air for 30 min.

the results showed that oxygen related defect density was reduced after thermal annealing of ZnO NPs (Supporting Information Figure S1).

As this superhydrophobic coating can be effectively removed by heat treatment at elevated temperatures, the transition between superhydrophobicity and superhydrophilicity was studied by alternating heat treatment and SA coating (Figure 6). This process was repeated over 10 times and showed good reproducibility with only subtle changes in water contact angles, resulting in switchable wetting behavior between superhydrophobic and superhydrophilic wetting states.

The stability of the superhydrophobicity under dynamic conditions as well as under stationary conditions is an essential element for practical applications. To investigate the impact dynamics, a 9 μL water droplet with a diameter of 1.5 mm and velocity of 0.5 m/s was impinged on the as-prepared and stearic acid-modified ZnO NP films. As shown in the Figure 7a, the water droplet on the as prepared samples spreads immediately and permeates into the nanostructures. For stearic acid-treated samples, however, the water droplet did not soak into the valley but rather bounced (Figure 7b). The air pocket and capillary force supported the droplet throughout the droplet impact. These results indicate that our superhydrophobic surface is very stable in dynamic conditions such as being exposed to water drops or even in falling rain.

CONCLUSIONS

In summary, a facile fabrication method of a superhydrophobic nanocoating was investigated involving a simple spin-coating step followed by the chemisorption of a fatty acid. The resulting coating showed a tremendous water repellency (static water contact angle = 158°), and the water contact angle could be modulated by changing the number of deposition cycles of ZnO NPs. Varying the number of deposition cycles of ZnO NPs controlled the surface roughness and affected the surface wetting properties. This simple coating method can be universally applied to various substrates including rigid surfaces, flexible surfaces, papers, and cotton fabrics and thus effectively used in various potential applications. The superhydrophobic surface showed high thermal stability and could be switched to a superhydrophilic state through heat treatment with good reversibility. Also the dynamic stability of a stearic acid-treated ZnO NPs film was studied under impact dynamic conditions for practical applications.

ASSOCIATED CONTENT

Supporting Information. Water contact angle of fatty acid modified ZnO NP films as a function of the carbon number of fatty acids, water contact angle on flat surfaces without ZnO NPs measured before and after stearic acid treatment, and photoluminescence (PL) from ZnO nanoparticles before and after air annealing at 300 °C. This material is available free of charge via the Internet at http://pubs.acs.org.

AUTHOR INFORMATION

Corresponding Author
*E-mail: kyong@postech.ac.kr.

ACKNOWLEDGMENT

This work was supported by Samsung Electronics, POSCO, grants from the National Research Foundation (Grants NRF2010-0009545 and NRF2010-0015975), and by the Korean Research Foundation Grants funded by the Korean Government (MOEHRD) (Grant KRF-2008-005-J00501).

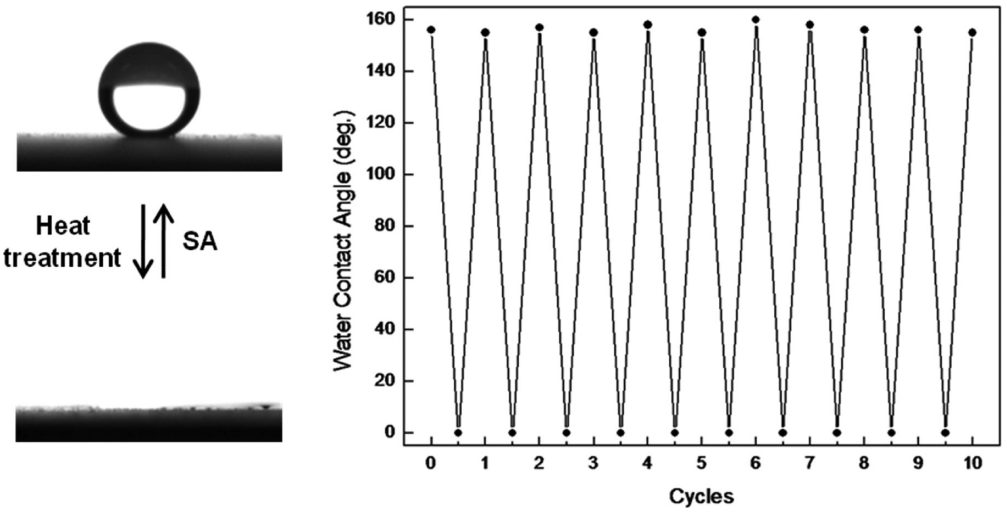

Figure 6. Reversible switching characteristics of the superhydrophobicity−superhydrophilicity transition of the SA-coated ZnO by alternating thermal treatment and SA coating.

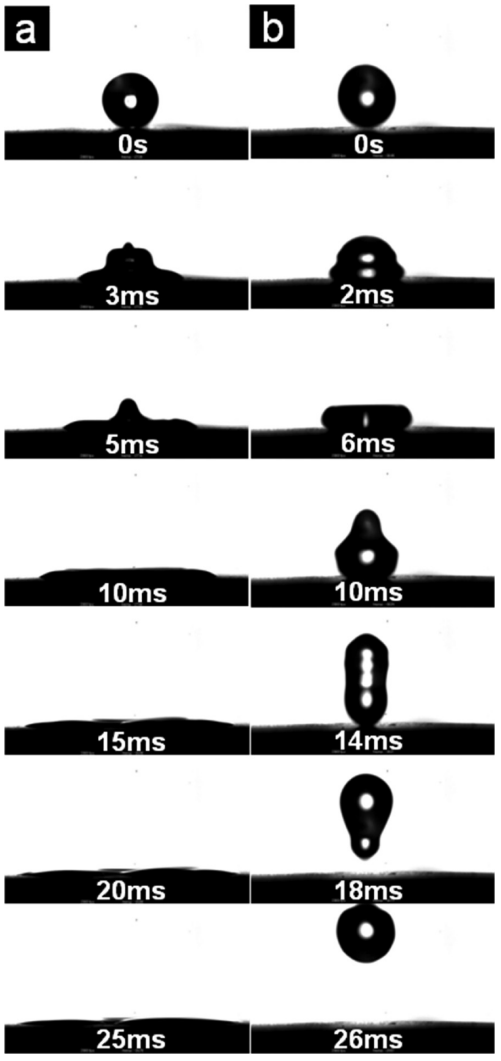

Figure 7. Sequential images of a water droplets impinging on the (a) as-prepared and (b) chemically modified ZnO coatings.

REFERENCES

(1) Niu, J. J.; Wang, J. N. *J. Phys. Chem. B* **2009**, *113*, 2909–2912.
(2) Meuler, A. J.; Smith, J. D.; Varanasi, K. K.; Mabry, J. M.; McKinley, G. H.; Cohen, R. E. *ACS Appl. Mater. Interfaces* **2010**, *2*, 3100–3110.
(3) Jiang, L.; Yao, X.; Li, H. X.; Fu, Y. Y.; Chen, L.; Meng, Q.; Hu, W. P.; Jiang, L. *Adv. Mater.* **2010**, *22*, 376–379.
(4) Gui, X. C.; Wei, J. Q.; Wang, K. L.; Cao, A. Y.; Zhu, H. W.; Jia, Y.; Shu, Q. K.; Wu, D. H. *Adv. Mater.* **2010**, *22*, 617–621.
(5) Zhang, J. L.; Han, Y. C. *Langmuir* **2009**, *25*, 14195–14199.
(6) Koch, K.; Bhushan, B.; Barthlott, W. *Soft Matter* **2008**, *4*, 1943–1963.
(7) Wang, L.; Zhang, X.; Fu, Y.; Li, B.; Liu, Y. *Langmuir* **2009**, *25*, 13619–13624.
(8) Kwak, G.; Seol, M.; Tak, Y.; Yong, K. *J. Phys. Chem. C* **2009**, *113*, 12085–12089.
(9) Feng, X.; Feng, L.; Jin, M.; Zhai, J.; Jiang, L.; Zhu, D. *J. Am. Chem. Soc.* **2003**, *126*, 62–63.
(10) Pauporté, T.; Bataille, G.; Joulaud, L.; Vermersch, F. J. *J. Phys. Chem. C* **2010**, *114*, 194–202.
(11) Feng, X.; Zhai, J.; Jiang, L. *Angew. Chem., Int. Ed.* **2005**, *44*, 5115–5118.
(12) Sun, W.; Zhou, S.; Chen, P.; Peng, L. *Chem. Commun.* **2008**, *5*, 603–605.
(13) Bauer, S.; Park, J.; Mark, K. v. d.; Schmuki, P. *Acta Biomater.* **2008**, *4*, 1576–1582.
(14) Kwak, G.; Lee, M.; Yong, K. *Langmuir* **2010**, *26*, 9964–9967.
(15) Wang, S.; Feng, X.; Yao, J.; Jiang, L. *Angew. Chem., Int. Ed.* **2006**, *45*, 1264–1267.
(16) Kwak, G.; Lee, M.; Senthil, K.; Yong, K. *Langmuir* **2010**, *26*, 12273–12277.
(17) Niu, J. J.; Wang, J. N. *J. Phys. Chem. B* **2009**, *113*, 2909–2912.
(18) Lu, S. H.; Ni Tun, M. H.; Mei, Z. J.; Chia, G. H.; Lim, X.; Sow, C.-H *Langmuir* **2009**, *25*, 12806–12811.
(19) Misra, A.; Giri, J.; Daraio, C. *ACS Nano* **2009**, *3*, 3903–39089.
(20) Sethi, S.; Dhinojwala, A. *Langmuir* **2009**, *25*, 4311–4313.
(21) Ming, W.; Wu, D.; van Benthem, R.; de With, G. *Nano Lett.* **2005**, *5*, 2298–2301.
(22) Tsai, H.-J.; Lee, Y.-L. *Langmuir* **2007**, *23*, 12687–12692.
(23) Bravo, J.; Zhai, L.; Wu, Z.; Cohen, R. E.; Rubner, M. F. *Langmuir* **2007**, *23*, 7293–7298.
(24) Yildirim, A.; Budunoglu, H.; Daglar, B.; Deniz, H.; Bayindir, M. *ACS Appl. Mater. Interfaces* **2011**, *3*, 1804–1808.

(25) Ke, Q.; Fu, W.; Wang, S.; Tang, T.; Zhang, J. *ACS Appl. Mater. Interfaces* **2010**, *2* (8), 2393–2398.
(26) Zhang, J.; Pu, G.; Severtson, S. J. *ACS Appl. Mater. Interfaces* **2010**, *2*, 2880–2883.
(27) Kwak, G.; Yong, K. *J. Phys. Chem. C* **2008**, *112*, 3036–3041.
(28) Wenzel, R. N. *Ind. Eng. Chem.* **1936**, *28*, 988–994.
(29) Cassie, A. B. D.; Baxter, S. *Trans. Faraday Soc.* **1944**, *40*, 546–551.